

19th Annual Intelligent Ground Vehicle Competition

Georgia Institute of Technology – RoboJackets

Design Report: Roxi

Joeseeph Hickey

John Madden

Stefan Posey

Jacob Schloss

May 10, 2011

Abstract

abstract lorem ipsum

Contents

1	Introduction	5
1.1	RoboJackets	5
1.2	Team Members	5
2	Overall Design	6
3	Mechanical Design	7
3.1	Structure Overview	7
3.2	Drive System	8
3.3	Waterproofing	8
3.4	Electronics Accommodation	8
4	Electronics Design	10
4.1	Sensors	10
4.2	Power	11
4.3	Computers	12
4.4	Safety Features	12
5	Software Design	14
5.1	Architecture	14
5.2	Algorithms	14
6	Performance	18
	References	19

List of Figures

1	Power Schematic	11
2	Raw Camera Frame	14
3	Transformed Camera Frame	14
4	Color Segmentation Output	15
5	Feature Tracker Output	16
6	World Map	16

List of Tables

1	2011 RoboJackets / IGVC Team	5
---	--	---

1 Introduction

1.1 RoboJackets

RoboJackets is an robotics competition and outreach group that has been operating at the Georgia Institute of Technology since 1999. Overall the RoboJackets consist of four teams a FIRST outreach / mentorship, Middle Weight BattleBots, RoboCup Small Size and IGVC. In all members come from many of the engineering departments across campus (prominently Mechanical, Aerospace, Electrical, and Computer Science) thus providing a truly multidisciplinary robotics development experience. The RoboJackets IGVC Team initially started in 2004 has fielded a team every year except 2005 and has been able to attain a top ten finish in the autonomous course since 2007. This past January, the RoboJackets along with the entire Student Competition Center moved to a new off campus facility. The move in total represented a loss of nearly two months of work, but given this many upgrades were still undertaken.

1.2 Team Members

The 2011 team members are listed in Table 1.

Table 1: 2011 RoboJackets / IGVC Team

Name	Degree / Class	Role
Joe Hickey	BS Mechanical Engineering / Sophomore	Mechanical design and build
John Madden	BS Mechanical Engineering and Computer Science/ Senior	Project Manager, Mechanical build, Software
Kenneth Marino	BS Electrical Engineering / Sophomore	Software, Electronics
Stefan Posey	BS Aerospace Engineering / Senior	Mechanical build
Jacob Schloss	BS Aerospace Engineering / Senior	Software, Electronics
Akshay Srivastava	BS Aerospace Engineering / Junior	Electronics

2 Overall Design

3 Mechanical Design

3.1 Structure Overview

Following our move last year to a four wheeled drive base, our team sought to further improve on this platform which provided a large increase in manoeuvrability and space efficiency over our previous model. During system debrief and review, several actionable deficiencies and areas of improvement for last years mechanical platform were noted. These included poor suspension performance, high weight, waterproofing issues, and lack of a payload restraining system that would handle the new increased speed limit. This years' drive base was guided by the following main goals:

1. Increased waterproofing performance
2. Outer panel simplification
3. Reduction in overall mass
4. Improved payload accommodation
5. Ability to hold a new laptop
6. Enhanced ride characteristics for higher top speed

To this end a new mechanical platform has been developed which features a more robust exterior panelling system, a lighter weight construction, improved electronics accommodation, and a low cost suspension. The previous three zone layout has been maintained with the structure being composed of a front, middle, and rear zone. Their content is as follows:

1. Front: Forward LIDAR, Motors, GPS, & Power support for laptop
2. Middle: Main Batteries, Motor Drive Electronics, & Power Distribution
3. Rear: Laptop, Camera, Rear LIDAR, GPS, Button Panel, & Safety Light

The frame is constructed out of 1/16" wall 1" sq. steel tube and aluminium panels. Much of the assembly was accomplished with MIG welding and the use of 1/4-20 fasteners. The outer cover is again made from polycarbonate panels which have a new attachment method that aides in rain-proofing. Overall the new system has retained many of the improvements made last year while adding key enhancements which are presented here in.

3.2 Drive System

Motor Layout & Suspension

As with last year our platform features an independently suspended four wheel drive system. Previously our suspension system was made with spare air pistons coupled with springs. These provided marginal ride smoothing, and worked well enough for our systems slow pace. In designing a new shock absorber system, our team consulted with the FormulaSAE and BajaSAE team which we share our shop with to gain a better understanding of the shocks they utilize and what characteristics we were looking for in our system. With cost in mind we purchased some dampers for riding lawn mower seats and modified them by adding springs to their stroke. These custom shocks have become a simple yet highly costs effective solution for our needs. A close up of one of these shocks can be seen on in the CAD rendering and picture in Figure X.

Motors & Encoder Modification

As with last year, this years base is powered by four NPC T64 brushed motors. Each motor has a custom adapter plate and shaft mounted on the rear for attaching a US Digital encoder. These encoders allow for independent control of each motor by the electronics system presented later in this paper. Figure X shows the rear of a modified motor with the attached encoder.

3.3 Waterproofing

3.4 Electronics Accommodation

Laptop

One of the biggest improvement to our system this year is a new laptop which moved us from our 6 year old Pentium M powered laptop to an i7 powered machine. This new laptop is larger than the previous one which prompted a reworking of the front and rear. In the end the previous year direct desk style access was attained. This year side panels were added around the laptop to reduce sun glare and enhance screen readability during field testing. The improved usability of this area and previously mentioned rain-proofing have add much to the system.

Camera

LIDAR

The modified SICK NAV 200 LIDARs are mounted in the front and rear of the vehicle and each have an unobstructed sweep of roughly 255 degrees. The LIDARs are protected above from rain by overhangs which also serve as compartments for the laptop and laptop power system. The units

are attached to the base through an intermediate aluminium plate. This allows them to be removed from the vehicle with only loosening three 1/4-20 bolts which are the standard fastener for our platform.

Interface Panel

Power Electronics

4 Electronics Design

The electronics for Roxi can be broken into three major categories: Senors, Power, and computers.

4.1 Sensors

Roxi uses vision and LIDAR as its primary sensors used for the navigation challenge and also has GPS and wheel encoders to allow for waypoint navigation.

4.1.1 Vision

The vision system consists of a AVT Guppy F-036C camera connected via an IEEE 1394a link to the main computer. This camera is capable of 752 x 480 resolution at 64 fps. This camera is polled at approximately 10 Hz to send a new frame to the vision algorithm. The camera is placed at the top of the mast, facing forwards and down to allow the lines and obstacle in front of the robot to be sensed.

4.1.2 Wheel Encoder

Each wheel is connected to a quadrature wheel encoder, allowing wheel rate to be measured. This allows the velocity of the robot to be measured. The encoder is a US Digital E3-200-375-I-H-M-B, with 200 counts per revolution and an index channel. This allows for wheel rates up to XX speed to be sensed. The quadrature lines drive interrupts on a microcontroller, which then feeds the state of the lines to a state machine which increments or decrements a wheel counter. Wheel angular velocity is measured by differencing the number of counts over a 5 ms period, allowing a bandwidth of XX Hz and XX m / s. The microcontrollers are capable of sending both rate and count information to the laptop, allowing for speed control and odometry operations.

4.1.3 LIDAR

Two front and rear mounted Sick NAV300 LIDAR are used as object and ramp detectors. The LIDAR have a 270° FOV and a 10 meter range. The front facing LIDAR is used as an object finder, while the back facing LIDAR is used as a safety feature allowing the robot to sense if an object / person is moved behind it after the robot has moved through an area.

4.1.4 GPS

A GPS is used to provide world position to the robot, allowing obstacles to be placed in world space and allowing waypoints to be followed. A Garmin “GPS 18-5Hz” gps is mounted to the

mast to allow a clear view of the sky. This GPS is accurate to $< 15 \text{ m} / < 3 \text{ m}$ (GPS / WAAS) and has a time to first fix of 45 seconds. The GPS updates 5 times per second.

4.2 Power

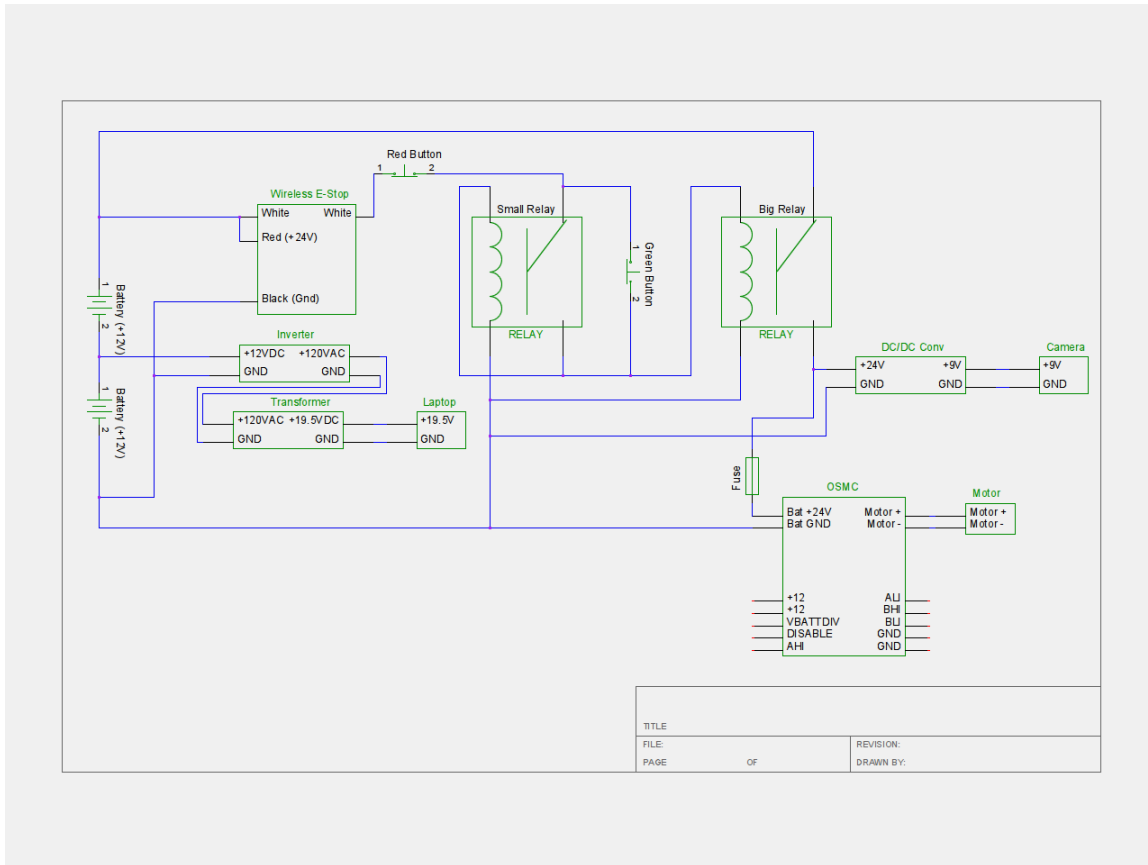


Figure 1: Power Schematic

4.2.1 Main Power

Main power for the robot comes from two sealed lead acid gell-cell batteries. These batteries are connected in series to produce a nominal 24 VDC supply for the motors and other systems. This provides approximately $XX \text{ W} \cdot \text{hr}$ of energy, XX hours of runtime of the motors, and XX hours of runtime of the electronics and motors.

The batteries are connected to a power distribution board, which allows the connection to each motor to be fused with XX Amps, allowing power to be cut in the event of a motor stall to prevent damage to the H-bridge. Power is also provided to several DC-DC boost converters, which output 5 VDC, 9 VDC, and 19.5 VDC for other electronics on the robot.

4.2.2 H Bridge

Each motor is connected to an OSMC H-bridge. This board is used to allow a low power signal from the microcontrollers to generate a high power PWM input to the motors. Each OSMC is capable of switching up to 50 VDC at 160A cont / 300A peak, allowing significant margin above our standard operating power of around 24 VDC / 20 A.

4.2.3 Component Power

Other systems are provided power through the use of DC-DC converters to produce voltages at 5 V, 9 V, and 19.5 V. This allows for the usb tethered microcontrollers, the sensors, and the main computer to be powered off of the main lead acid batteries. This greatly simplifies charging the robot, as only one battery system needs to be maintained.

4.3 Computers

4.3.1 Main Computer

Nearly all computation is performed on a single laptop containing a quadcore Intel Core i7 cpu, cuda enabled NVIDIA 285M gpu, and 6 GB of RAM. This computer is responsible for all vision, LIDAR, and GPS data processing and all path planning and control algorithms. It also forms the core of the sensor interconnects, providing the firewire and USB bus the camera, GPS, and microcontrollers use. This laptop replaces the main computer used in previous years, and was replaced with support from Northrup Grumman.

4.3.2 MCU

Microcontrollers are used on Roxi as data acquisition boards to collect data from the wheel encoders, and as motor control boards to generate PWM signals to drive the H-bridges. There are 6 ATmega328p based Arduino Duemilanove boards on the robot, 4 interfacing with the wheel encoders, and 2 to drive the motors.

4.4 Safety Features

As autonomous systems are dangerous, and can behave unpredictably when hardware or software errors occur, several safety features are included in this robot.

4.4.1 Emergency Stop

The robot is equipped with an emergency stop that when triggered will physically disconnect power to the motors. This will stop forward motion quickly. Both a physical button on the back of the robot and a wireless trigger are provided.

4.4.2 Safety Light

4.4.3 Rear-Facing LIDAR

This robot also uses a rear facing LIDAR as a safety feature. This allows the robot to sense if something has moved behind it, allowing the robot to avoid hitting anyone walking behind it if the robot decides to move backwards during autonomous operation.

5 Software Design

5.1 Architecture

The software on the robot is split between algorithmic and control code that runs on the primary laptop and data acquisition code that runs on the microcontrollers. This allows the laptop to perform all of the intensive calculation allowing the use of very cheap microcontrollers that only need to perform basic low level actions.

The primary language in our system is C++. Object oriented approaches are used for programs that run on the laptop, while simplified imperative code is used on the microcontrollers to minimise overhead. Several standard system and computer graphic libraries are used in our code base. The Boost c++ library is used extensively to provide data structures, serial IO handlers and threads. Image processing is mostly done with algorithms built from elements provided by OpenCV, with some transforms offloaded to the GPU with OpenGL. The codebase currently only runs on linux, however with out migration to Boost we could theoretically port the code base to run on other major platforms (Windows, MacOS, Solaris) with little effort.

5.2 Algorithms

5.2.1 Vision

The robot uses vision as the primary method of detecting obstacles and lines. The vision algorithm has been developed and modified over several years of competition and is considered reasonably robust. After passing the input video through several different algorithms, a short-term map of the world is created, which the robot is driven off of.



Figure 2: Raw Camera Frame



Figure 3: Transformed Camera Frame

The input video, Figure 3, is first passed through an inverse perspective transform, as seen above-right. This transform makes both near and far off objects a normalized size, and makes

the image appear to be taken from directly overhead. This flattened image assumes the course is a plane, which does cause distortion of the barrels, but this is accounted for in the mapping algorithm. The transformed image is much easier to process into a map than a normal, perspective image would be.

The images is then color segmented and thresholded based on the color that is centered directly in front of the robot, as seen above. Safe colors are marked white, the rest are black. The color is averaged in time between frames to allow for some variation in color, for example, if there is dead pach in the grass. This allows the robot to operate on many different surfaces with the same software. For testing we have operated on asphalt parking lots, navigating between the lines marking parking spaces.

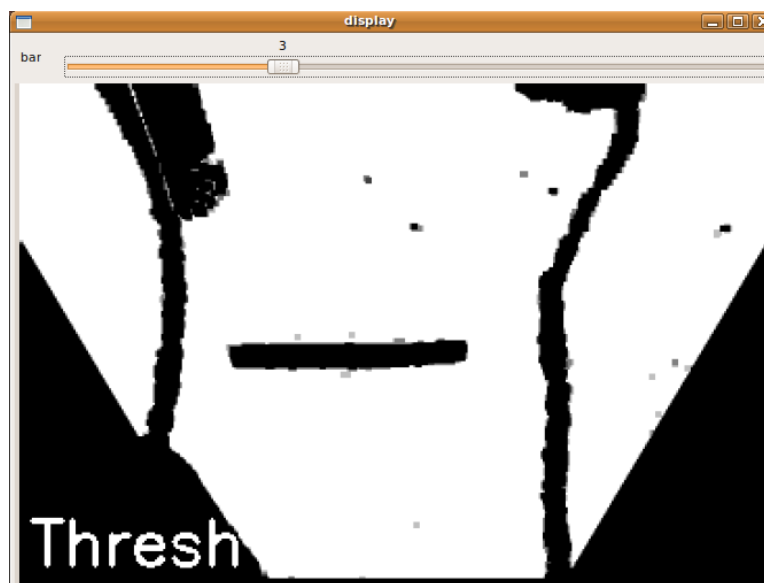


Figure 4: Color Segmentation Output

After converting the transformed image to grayscale, feature tracking is preformed between subsequent frames. The tracked features are denoted by the black lines in the above grayscale image. The algorithm looks for features that have been translated and rotated between frames. This allows us to build a set of likely homographic transform between the images, which can be backed out into likely robot motion between frames. The possible homographic transforms often include several incorrectly matched points, so RANSAC, a nonlinear filter good at outlier handling, is used to reject the outliers and select the best transform.

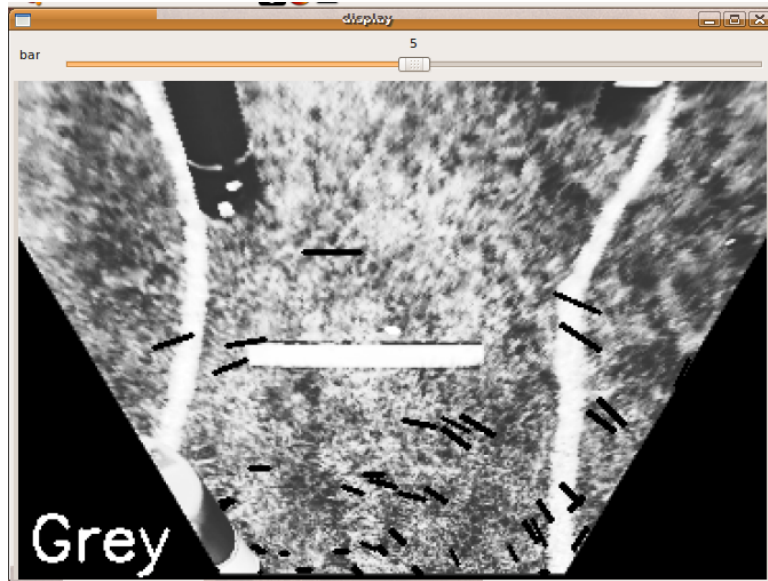


Figure 5: Feature Tracker Output

Using motion data, camera frames are drawn into the world map, shown to the right above. The map is a grayscale image, representing a probability function of traversability, where black (0) represents non-traversable, gray (127) represents unknown areas and white (255) represents traversable areas. The map is built up as the robot moves, and slowly decays back to gray to prevent loop closure errors from building up. This map allows the robot to remember that it just passed an obstacle and needs to not turn sharply in order to avoid a collision. The robot is driven from the map, by a path planning algorithm.

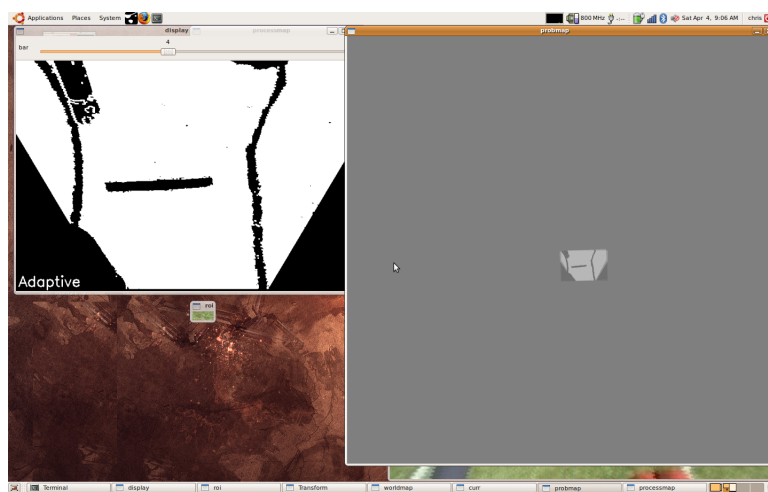


Figure 6: World Map

5.2.2 Path Planning

Once the world map is generated, a potential fields algorithm is used. The robot is attracted to the furthest clear point in view and the ramp for the autonomous challenge and the nearest waypoint for the navigation challenge. Obstacles repel the robot, and the strength of the field is higher if the object is closer.

5.2.3 Sensor Filtering

As our robot has 2 GPS modules, we perform basic filtering to allow the error in the position measurement to be reduced. At this time, a simple average is performed which theoretically reduces random error by a factor of 1.41. We plan to extend this to a full Kalman filter incorporating data from the GPS, wheel encoders, and an IMU (currently not integrated) in future competitions.

5.2.4 LIDAR

The LIDAR is used as an obstacle and ramp detection sensor. The incoming range information is filtered with a running average to reduce random noise, and is then passed through an erosion-dilation filter to remove isolated points. The 2^{nd} derivative is then calculated and thresholded to look for linear objects similar in width to the ramp which when found are given to the path planner as a special goal. Returns with non-zero 2^{nd} derivatives are interpreted and given to the path planner as objects to be avoided.

6 Performance

References

- [1] *Space Network User's Guide*, pages 35–257, 317–327, 365–389. Number 450-SNUG. NASA GSFC, 9th edition, August 2007.
- [2] Advanced Scientific Concepts Inc. *DragonEye 3D Flash LIDAR Space Camera*. <http://advancedscientificconcepts.com/products/dragoneye.html>.
- [3] Allied Vision Technologies. *Big Family*.
- [4] Allied Vision Technologies. *Prosilica GE4900 Datasheet*, v2.0.1 en edition.
- [5] G. Richard Curry. *Radar Systems Performance Modeling*. Artech House Publishers, 2004.
- [6] Zhaoxu Dong. *Mechanical Behavior of Silica Nanoparticle Impregnated Kevlar Fabrics*. PhD thesis, Purdue University, 2008.
- [7] Du Pont. *Technical Guide Kevlar Aramid Fiber*.
- [8] European Space Agency. *New Radar Satellite Technique Sheds Light on Ocean Current Dynamics*. http://www.esa.int/esaEO/SEMZRQEMKBF_economy_0.html.
- [9] European Space Agency. *Sentinel-1*. http://www.esa.int/esaLP/SEMBRS4KXMF_LPgmes_0.html.
- [10] Navid S. Fatemi, Howard E. Pollard, Hong Q. Hou, and Paul R. Sharps. Solar Array Trades Between Very High-Efficiency Multi-Junction and Si Space Solar Cells. pages 2–3. Emcore Photovoltaics, September 2003.
- [11] Christophe Geuzaine and Jean-Francois Remacle. Gmash: A three dimensional finite element mesh generator with built-in pre- and post- processing facilities. *International Journal for Numerical Methods in Engineering*, 79(11):1309–1331, 2009.
- [12] Honeywell. *M50 Controll Moment Gyroscope*, 7th edition, January 2006.
- [13] Jorgen Jensen and George Townsend, editors. *Orbital Flight Handbook, Part 1 - Basic Techniques and Data*, volume 1 of *Space Flight Handbooks*, pages V–52. Martin Company Space Systems Division, 1967.
- [14] Bassem Mahafza. *Radar Systems Analysis and Design Using MATLAB*. Chapman and Hall, 2005.
- [15] Malin Space Science Systems. *ECAM-C50*.

- [16] Malin Space Science Systems. *ECAM-DVR4*.
- [17] Malin Space Science Systems. *ECAM-IR1*.
- [18] Malin Space Science Systems. *ECAM Optics*.
- [19] et al Mikhalaylovskiy, Yuriy. *Impact*. <http://impact.sourceforge.net/>.
- [20] PRC Laser Corp. *FH Series High Power Lasers*, 2005.
- [21] Ramsey Electronics. *The 'LOGI' Log Periodic Antenna*.
- [22] Mark A. Richards. *Fundamentals of Radar Signal Processing*. McGraw-Hill, 2005.
- [23] Wolfgang O. Schall. Orbital derbis removal by laser radiation. *Acta Astronautica*, 24:343–351, 1991.
- [24] Merrill Skolnik. *Introduction to Radar Systems*. McGraw-Hill, 2002.
- [25] SpaceX. *Falcon 1 Launch Vehicle Payload User's Guide*, 7th edition, May 2008.
- [26] SpaceX. *Falcon 9 Launch Vehicle Payload User's Guide*, 1st edition, 2009.
- [27] John F. Stocky and Christopher M. Stevens. Guidelines for preparing project risk management plans. Technical report, NASA, 2005.
- [28] J.D. Weinberg, R. Craig, P. Earhart, I. Gravseth, and K.L. Miller. Flash lidar systems for hazard detection, surface navigation and autonomous rendezvous and docking. page 1. Ball Aerospace & Technologies Corp., 2007.
- [29] James R. Wertz and Wiley J. Larson, editors. *Space Mission Analysis and Design*, pages 301–497, 894–897. Microcosm Press and Springer, 3rd edition, 2008.